Strain-induced fundamental optical transition in (In,Ga)As/GaP quantum dots

C. Robert,[1,a)] M. O. Nestoklon,[2] K. Pereira da Silva,[3,4] L. Pedesseau,[1] C. Cornet,[1] M. I. Alonso,[3] A. R. Goñi,[3,5] P. Turban,[6] J.-M. Jancu,[1] J. Even,[1] and O. Durand[1]
[1]*Université Européenne de Bretagne, INSA Rennes, France and CNRS, UMR 6082 Foton, 20 Avenue des Buttes de Coësmes, 35708 Rennes, France*
[2]*Ioffe Physico-Technical Institute, Russian Academy of Sciences, 194021 St. Petersburg, Russia*
[3]*ICMAB-CSIC, Campus UAB, 08193 Bellaterra, Spain*
[4]*Departamento de Física, Universidade Federal do Ceará, P.O. Box 6030, Fortaleza–CE, 60455-970, Brazil*
[5]*ICREA, Passeig Lluís Companys 23, 08010 Barcelona, Spain*
[6]*Equipe de Physique des Surfaces et Interfaces, Institut de Physique de Rennes UMR UR1-CNRS 6251, Université de Rennes 1, F-35042 Rennes Cedex, France*

(Received 18 November 2013; accepted 22 December 2013; published online 9 January 2014)

The nature of the ground optical transition in an (In,Ga)As/GaP quantum dot is thoroughly investigated through a million atoms supercell tight-binding simulation. Precise quantum dot morphology is deduced from previously reported scanning-tunneling-microscopy images. The strain field is calculated with the valence force field method and has a strong influence on the confinement potentials, principally, for the conduction band states. Indeed, the wavefunction of the ground electron state is spatially confined in the GaP matrix, close to the dot apex, in a large tensile strain region, having mainly Xz character. Photoluminescence experiments under hydrostatic pressure strongly support the theoretical conclusions. © *2014 AIP Publishing LLC*.
[http://dx.doi.org/10.1063/1.4861471]

The development of nanostructures on GaP has been extensively studied for the past decade to meet the needs for an efficient light emitter/absorber on Si substrates. Indeed, thanks to the small lattice-mismatch between GaP and Si (0.37% at 300 K), the coherent growth of a low defect density GaP buffer layer onto Si(001) substrate has been demonstrated by several groups,[1–4] opening the route towards a relevant platform for the development of reliable optoelectronic devices compatible with nowadays Si technology. Among the nanostructures grown on GaP substrates and/or GaP/Si pseudo substrates, dilute nitride quantum wells (QW) (GaAsPN and InGaPN) appear among the most reported in the literature.[5–7] Nevertheless, further optimization is still required to decrease the threshold current densities in the laser devices based on such nanostructures (4 kA.cm^{-2} in pulsed mode at 300 K on GaP substrate[8] and 4.4 kA.cm^{-2} in pulsed mode at 120 K on Si substrate[9]).

Quantum dot (QD) based active zones offer a reliable alternative to QW-based laser structures, as it may take advantage of the lower dimensionality to reduce the threshold current densities. In this way, the InGaAs/GaP QD system has recently attracted much attention. If the first report on metalorganic chemical vapor deposition (MOCVD) grown InGaAs/GaP QD already takes back ten years,[10] the major progresses have been achieved in the last three. MBE-growth of low density $In_{0.5}Ga_{0.5}As$ QD was reported in 2010.[11] The first room temperature photoluminescence (PL) was measured in 2011 from high QD density[12] and single QD type-I emission from $In_{0.5}Ga_{0.5}As$/GaP QD was obtained in 2012.[13] Room temperature electroluminescence has been demonstrated recently on both GaP substrate[14] and Si substrate.[15] Meanwhile, the QD structural properties have been analysed by both plane-view[16] and cross sectional scanning-tunneling microscopy (STM).[17] The issue of InGaAs/GaP QD electronic band structure has also been raised. First, Fukami *et al*. have calculated the heavy hole (HH) and electron quantum levels at the Γ point with a simple model-solid theory approach and pointed out the proximity of the Γ electron confined state with the X conduction band of GaP.[18] This result was refined by calculating the first HH and electron state at the Γ point with an eight band **k**·**p** model.[16,19] In addition, the positions of the first confined states in the X and L valleys were deduced from an extended *spds* tight-binding (TB) model assuming a QW with a thickness equal to the height of the QD and disregarding the possible mixing between Γ, X, and L valleys.[16] From this mixed **k**·**p**/TB simulation, an indirect to direct crossover was predicted for the ground optical transition in large QD and for In content above 30%. Nevertheless, this simple model misses some important features, especially in the low In content range, where the proximity of both QD and barrier states has to be analysed carefully. In this work, we simulate a realistic GaAs QD buried in a GaP matrix with a full supercell tight binding model at the atomistic level. The simulation results are supported by pressure dependent PL experiments on an (In,Ga)As/GaP QD sample with a low In content.

The extended *spds* tight binding model is a state of the art atomistic simulation method able to describe the electronic band structure throughout the entire Brillouin zone of bulk semiconductors and heterostructures. We use the TB parameters determined in Ref. 20, which are known to reproduce well the experimental band gaps and the effective masses of the main cubic bulk semiconductors. Thanks to

[a)]Electronic addresses: cedric.robert@insa-rennes.fr and cedric.robert@tyndall.ie.

their excellent transferability, they have been demonstrated to correctly describe more complex structures such as indirect band gap heterostructures,[21] short-period superlattices,[22] impurity states,[23] and surfaces.[24] The simulation of embedded QD has also been demonstrated[25] although it adds the computational difficulty of the broken translational symmetry which often requires dealing with a large number of atoms. Indeed, the typical dimensions of a QD are around a few nanometers in height and a few 10 nm in diameter corresponding to a total of about 10^5 atoms. Moreover, the barrier material in which the QD is embedded has also to be considered, leading to a supercell size containing a few millions atoms. Dealing with a high number of atoms (up to 10^8) has been possible since recently thanks to the huge advances in massively parallel high performance computing.[26,27] In this letter, we limit the size of the supercell to about one million in order to perform the TB computation feasible on a moderately parallel 12 CPUs machine.

One of the advantages of the fully atomistic supercell TB model is that it does not require any approximation on the QD shape leading to simulations using very realistic geometries, provided, for instance, by STM with atomic resolution.[16] The dimensions of the chosen QD are extracted from the plane-view STM image published in Ref. 16 and are summarized in Fig. 1. Since the capped QD generally do not exhibit a sharp edge at the apex as the one observed in plane-view STM, the simulated QD is truncated at a height of 3.4 nm, leaving a small flat surface at the top of the QD as suggested by X-STM images.[17,28] Finally, a 1 monolayer (ML) thick wetting layer (WL) is added to the supercell to account for the Stranski-Krastanov mode. The issues of indium content and its spatial inhomogeneity require a specific investigation as the one of Prohl *et al.* with X-STM fine analysis.[17] In order to compare the simulation results with our experimental results on (In,Ga)As/GaP QD displaying low In content (below 15%),[16] we choose to simulate a pure GaAs/GaP QD assuming similar morphology. The effect of In content will be discussed separately at the end of this letter. The GaAs QD and the WL are embedded in a

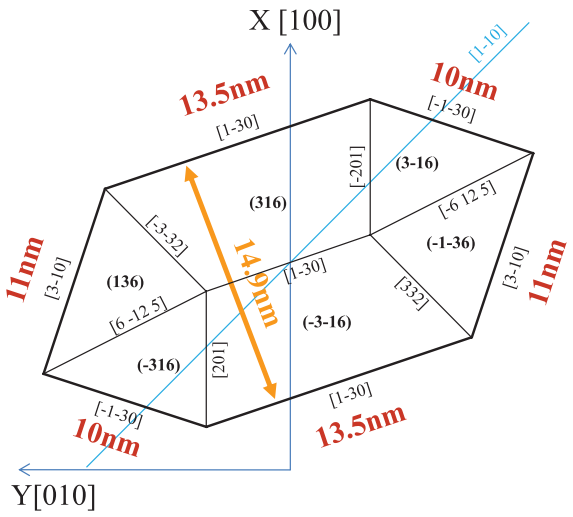

FIG. 1. Geometry of the GaAs/GaP QD for the TB simulation as measured on the plane-view STM image of Ref. 16. The QD height is truncated at 3.4 nm according to X-STM image of a buried QD.[28]

GaP supercell with a lateral size of 132 square MLs (around 36×36 nm^2) equivalent to a QD areal density of 7.7×10^{10} cm^{-2}. The height in the [001] direction is 86 MLs accounting for a GaP buffer layer below and a GaP cap layer above the QD with both thicknesses roughly equal to three times the QD height.

An initial supercell is first built with all atoms, regularly placed on the sites of an unstrained zinc-blende structure with the GaP lattice constant. The atomic positions are then relaxed with a valence force field (VFF) method[29] using two parameters to fit the C_{11} and C_{12} macroscopic elastic constants of both GaAs and GaP,[30] while committing a small error on the C_{44} values. This procedure has been demonstrated to be relevant for [001] grown QD.[31] The boundary conditions are periodic along the three supercell basis vectors. To model the biaxial strain imposed by the substrate, the two in-plane supercell basis vectors are set fixed during the VFF relaxation and the out-of-plane component is able to relax. Fig. 2(a) shows the calculated hydrostatic and biaxial strain components along the [001] direction through the QD centre. The strain field vanishes when going away from the QD, indicating that the GaP buffer thickness is enough to avoid vertical strain coupling between adjacent supercells. Both hydrostatic and biaxial strain components are found negative inside the QD in agreement with the expected result for a compressively strained QD. Furthermore, the biaxial part is significantly positive in the vicinity of the QD, especially in the GaP region at the apex of the QD.

Before reporting the confined electron and hole states for this supercell computation, it is interesting to use a simple and didactic representation of confinement potentials, to solely understand the role of the strain field. Fig. 2(b) shows the potentials in the Γ, X, and L conduction valleys as well as the HH and light hole (LH) potentials along the [001] direction through the QD centre calculated with the linear deformation potential theory.[32,33] Only the effects of the hydrostatic and biaxial strain components are considered in this simplified representation. We clearly see that the band alignment should favour a strongly confined HH state inside the QD, as predicted in previous theoretical studies.[16,18] Concerning the conduction valleys, the Γ potential is found to be well above the X potentials which confirms the impossibility of obtaining a Γ-type ground electron state inside the QD in the low In content range.[16] The case of X valleys is the most interesting. Due to the negative biaxial strain inside the QD, the X_{XY} and X_Z potentials are split with a downward shift of the X_{XY} component. In the GaP matrix surrounding the QD, the situation is reversed: because of the positive (tensile) biaxial component, a shallow X_Z confinement potential is present at the apex and at the base of the QD. It is important to notice that this shallow X_Z confinement potential could not be considered in previous theoretical studies,[16,18] because it requires to use a model taking into account both QD geometry and lateral conduction bands.

After having highlighted the band alignment issue, we present the results of the TB simulation of both hole and electron ground states in this supercell. The Hamiltonian eigenvalues are calculated combining a Lanczos algorithm[34] with a folded spectrum method.[35,36] The Coulomb interaction, leading to exciton formation, is not taken into account

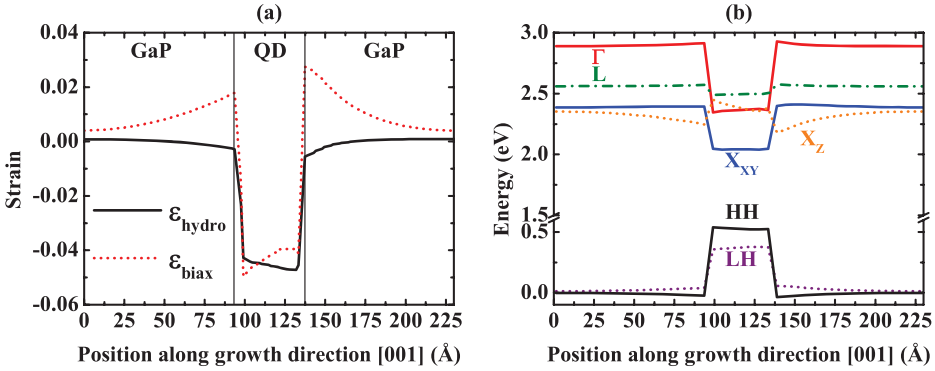

FIG. 2. (a) Hydrostatic ($\varepsilon_{hydro} = \varepsilon_{xx} + \varepsilon_{yy} + \varepsilon_{zz}$) and biaxial ($\varepsilon_{biax} = {}^1/_2(\varepsilon_{xx} + \varepsilon_{yy}) - \varepsilon_{zz}$) strain components along the z [001] direction through the GaAs/GaP QD centre. (b) Confinement potentials along the z [001] direction through the QD centre calculated with the linear deformation potential theory using the hydrostatic and the biaxial strain components. Calculations are performed at 0 K.

in this study. Fig. 3(a) shows that the ground hole level wave function is confined inside the QD and located 458 meV above the valence band maximum (VBM) of unstrained bulk GaP, in good agreement with the simple 8×8 **k·p** calculation on QD with similar dimensions.[16] From the analysis of the wave function decomposition onto the orbitals of the *spds* basis, we may infer that 75% of the weight is carried by the p_x and p_y orbitals, whereas less than 4% is carried by the p_z orbital. It shows unambiguously that this state is predominant of HH type. Fig. 3(b) shows the ground electron level wave function. Interestingly, the wave function is not confined in the GaAs QD but at the top of the QD, in the GaP matrix, located 2.248 eV above the VBM and 119 meV below the conduction band minimum of unstrained bulk GaP. The decomposition of the wave function shows that the main part of the weight (90%) is on the p_z, d_{xy}, and d_{3z^2-r} orbitals. This state is predominant of X_Z type and related to the shallow confinement potential highlighted in Fig. 2(b). According to Fig. 2(b), a confined electron state should also exist in the X_{XY} potential of the QD. The TB simulation indeed predicts such a state located 62 meV above the ground electron state (not shown here), in good agreement with the estimation given in Ref. 16. The reduced quantum confinement effect on the X_Z-like state as compared to the X_{XY}-like state may be attributed to the smoother confinement potential profile in the GaP matrix and the stronger X-effective mass in GaP than in GaAs.[30] Such strain-induced interface localized states have also been predicted in InP/GaP QD[37–39] and SiGe/Si QD.[40–42] Nevertheless, it differs from a true type-II band alignment such as GaSb/GaAs QD[43] in which the electron wave function is delocalized in the whole GaAs barrier when the Coulomb interaction is not taken into account.

To support this theoretical result, we present an experimental study of the dependence of the PL on external hydrostatic pressure. An (In,Ga)As/GaP QD sample, with one QD sheet layer and with low In content (typically below 15%, thus, below the indirect/direct crossover threshold) is analysed. Growth details are presented elsewhere.[12,16] Measurements are performed at room temperature employing a gasketed diamond anvil cell enabling to apply hydrostatic pressure up to 10 GPa. The sample is excited using a 405 nm line of a continuous wave laser diode and the PL signal is collected using a LabRam HR800 spectrometer equipped with a charge-coupled device detector. Additional descriptions of the pressure setup can be found in Ref. 44. Fig. 4 shows the PL spectra of (In,Ga)As/GaP QD for various values of hydrostatic pressure. The rough data are represented by thin lines. The interference fringes due to multiple reflections of the emitted light between both parallel-plane faces of the polished sample are readily observed. The thick lines represent the smoothed spectra. A first important result is the monotonic red-shift of the PL peak maximum with increasing pressure, which unambiguously proves that the PL peak involves X-type conduction states.[44] In first approximation, the expected pressure dependence for an X_Z-like level confined in GaP may follow the pressure dependence of the indirect band gap in GaP (-13 meV.GPa^{-1}).[45] This is actually what is observed in the inset of Fig. 4, where the energy of the PL peak maximum as a function of pressure is depicted (red circle points) and matches well with a pressure coefficient of -13 meV.GPa^{-1} (red line), supporting the theoretically predicted nature of the ground optical transition. Moreover, Fig. 4 also highlights the PL quenching with hydrostatic pressure. This results from the difference in compressibility between GaP and the QD

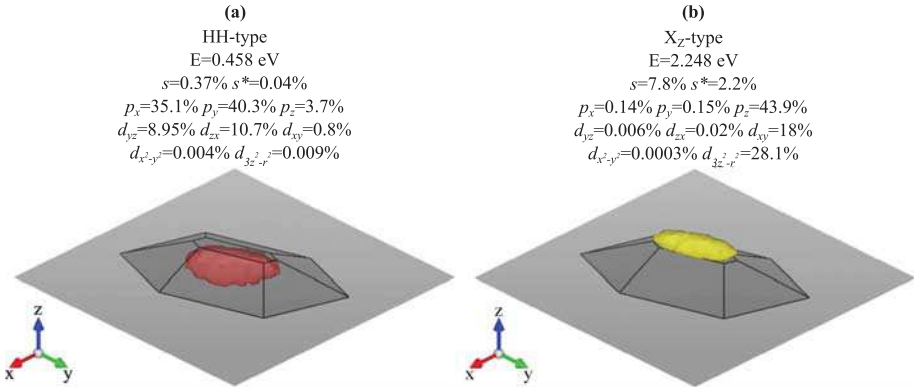

FIG. 3. (a) Ground hole state and (b) ground electron state calculated with the TB model in a GaAs/GaP QD at 0 K. The representation of wave functions considers volumes corresponding to 80% of the hole/electron densities. The wave function decomposition is indicated by a percentage on each orbital of the *spds* TB basis.

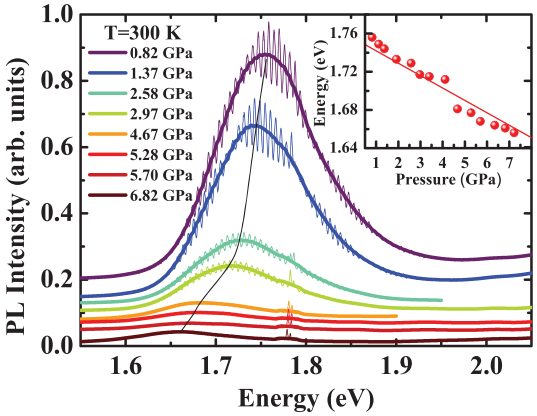

FIG. 4. Room temperature PL spectra of (In,Ga)As/GaP QD as a function of hydrostatic pressure. The rough data are shown by thin lines. The spectra are smoothed (thick lines) to avoid the interference fringes. The thin black line is a guide to the eye to highlight the variation of the energy of the maximum PL intensity, whose data points are plotted in the inset (red circle points). The red line displays the expected linear variation with a pressure coefficient of $-13\,\text{meV.GPa}^{-1}$.

material. Indeed, the bulk modulus of GaP (88 GPa) is higher than the bulk modulus of GaAs (75 GPa) and InAs (58 GPa).[46] Thus, when applying high hydrostatic pressure, the lattice-mismatch between the QD material and GaP decreases, leading to a reduction of the shallow X_Z potential shown in Fig. 2(b). The confinement of the electrons at the GaP barrier close to the apex of the QD is thus reduced with increasing pressure. The PL quenching may consequently be related to a more favourable escape of carriers into unstrained, extended zones of the GaP barriers.

In conclusion, we have thoroughly simulated a GaAs/GaP QD with a million atoms supercell *spds* tight binding code. The use of such a sophisticated model is mandatory to infer the nature of the ground electron state. Indeed, due to the strain field surrounding the GaP matrix, the wave function is found to be quantum confined in the GaP barrier almost at the apex of the QD. Pressure dependent PL experiments on low In content (In,Ga)As/GaP QD are in agreement with the electronic band structure computation. Finally, it is important to notice that the result presented in this letter does not question the prediction of an indirect to direct crossover occurring in large QD and for In content above 30%.[16] However, it shows that in the indirect region, the ground electron state is an X_Z-like state "mechanically" confined at the apex but outside the QD rather than being a X_{XY}-like state confined in the QD. Increasing In content below the indirect/direct crossover should even enhance this strain induced confinement as the lattice-mismatch between the QD material and GaP increases and consequently as the positive biaxial strain at the apex of the QD increases.

This research was supported by "Région Bretagne" through the PONANT project including FEDER funds. This work was also supported by the OPTOSI ANR Project No. 12-BS03-002-02 and the NANOTRANS C'NANO research program. This work has been performed using HPC resources of GENCI CINES, TGCC/CCRT, and IDRIS under the allocation 2013-[x2013096724]. K.P.S. acknowledges funding from the Brazilian CAPES agency through CGBE/BEX-Proc.6903-12-6 and the CNPq agency through grant-Proc. 142772/2010-0.

[1]K. Volz, A. Beyer, W. Witte, J. Ohlmann, I. Németh, B. Kunert, and W. Stolz, J. Cryst. Growth **315**, 37 (2011).
[2]T. J. Grassman, J. A. Carlin, B. Galiana, L.-M. Yang, F. Yang, M. J. Mills, and S. A. Ringel, Appl. Phys. Lett. **102**, 142102 (2013).
[3]K. Yamane, T. Kawai, Y. Furukawa, H. Okada, and A. Wakahara, J. Cryst. Growth **312**, 2179 (2010).
[4]T. Quinci, J. Kuyyalil, T. N. Thanh, Y. P. Wang, S. Almosni, A. Létoublon, T. Rohel, K. Tavernier, N. Chevalier, O. Dehaese, N. Boudet, J. F. Bérar, S. Loualiche, J. Even, N. Bertru, A. L. Corre, O. Durand, and C. Cornet, J. Cryst. Growth **380**, 157 (2013).
[5]B. Kunert, K. Volz, J. Koch, and W. Stolz, Appl. Phys. Lett. **88**, 182108 (2006).
[6]C. Robert, A. Bondi, T. Nguyen Thanh, J. Even, C. Cornet, O. Durand, J. P. Burin, J. M. Jancu, W. Guo, A. Létoublon, H. Folliot, S. Boyer-Richard, M. Perrin, N. Chevalier, O. Dehaese, K. Tavernier, S. Loualiche, and A. Le Corre, Appl. Phys. Lett. **98**, 251110 (2011).
[7]K. Umeno, S. M. Kim, Y. Furukawa, H. Yonezu, and A. Wakahara, J. Cryst. Growth **301–302**, 539 (2007).
[8]N. Hossain, S. J. Sweeney, S. Rogowsky, R. Ostendorf, J. Wagner, S. Liebich, M. Zimprich, K. Volz, B. Kunert, and W. Stolz, Electron. Lett. **47**, 931 (2011).
[9]S. Liebich, M. Zimprich, A. Beyer, C. Lange, D. J. Franzbach, S. Chatterjee, N. Hossain, S. J. Sweeney, K. Volz, B. Kunert, and W. Stolz, Appl. Phys. Lett. **99**, 071109 (2011).
[10]S. Fuchi, Y. Nonogaki, H. Moriya, A. Koizumi, Y. Fujiwara, and Y. Takeda, Phys. E (Amsterdam, Neth.) **21**, 36 (2004).
[11]Y. Song, P. J. Simmonds, and M. L. Lee, Appl. Phys. Lett. **97**, 223110 (2010).
[12]T. Nguyen Thanh, C. Robert, C. Cornet, M. Perrin, J. M. Jancu, N. Bertru, J. Even, N. Chevalier, H. Folliot, O. Durand, and A. Le Corre, Appl. Phys. Lett. **99**, 143123 (2011).
[13]K. Rivoire, S. Buckley, Y. Song, M. L. Lee, and J. Vučković, Phys. Rev. B **85**, 045319 (2012).
[14]Y. Song and M. Larry Lee, Appl. Phys. Lett. **100**, 251904 (2012).
[15]Y. Song and M. L. Lee, Appl. Phys. Lett. **103**, 141906 (2013).
[16]C. Robert, C. Cornet, P. Turban, T. Nguyen Thanh, M. O. Nestoklon, J. Even, J. M. Jancu, M. Perrin, H. Folliot, T. Rohel, S. Tricot, A. Balocchi, D. Lagarde, X. Marie, N. Bertru, O. Durand, and A. Le Corre, Phys. Rev. B **86**, 205316 (2012).
[17]C. Prohl, A. Lenz, D. Roy, J. Schuppang, G. Stracke, A. Strittmatter, U. W. Pohl, D. Bimberg, H. Eisele, and M. Dähne, Appl. Phys. Lett. **102**, 123102 (2013).
[18]F. Fukami, K. Umeno, Y. Furukawa, N. Urakami, S. Mitsuyoshi, H. Okada, H. Yonezu, and A. Wakahara, Phys. Status Solidi C **8**, 322 (2011).
[19]C. Robert, T. N. Thanh, C. Cornet, P. Turban, M. Perrin, A. Balocchi, H. Folliot, N. Bertru, L. Pedesseau, M. O. Nestoklon, J. Even, J.-M. Jancu, S. Tricot, O. Durand, X. Marie, and A. Le Corre, Nanoscale Res. Lett. **7**, 643 (2012).
[20]J.-M. Jancu, R. Scholz, F. Beltram, and F. Bassani, Phys. Rev. B **57**, 6493 (1998).
[21]J.-M. Jancu, R. Scholz, G. C. La Rocca, E. A. de Andrada e Silva, and P. Voisin, Phys. Rev. B **70**, 121306 (2004).
[22]M. Virgilio, G. Pizzi, and G. Grosso, J. Appl. Phys. **110**, 083105 (2011).
[23]M. O. Nestoklon, O. Krebs, H. Jaffrès, S. Ruttala, J.-M. George, J.-M. Jancu, and P. Voisin, Appl. Phys. Lett. **100**, 062403 (2012).
[24]J.-M. Jancu, J.-C. Girard, M. O. Nestoklon, A. Lemaître, F. Glas, Z. Z. Wang, and P. Voisin, Phys. Rev. Lett. **101**, 196801 (2008).
[25]M. Zieliński, M. Korkusiński, and P. Hawrylak, Phys. Rev. B **81**, 085301 (2010).
[26]G. Klimeck, S. S. Ahmed, H. Bae, N. Kharche, S. Clark, B. Haley, S. Lee, M. Naumov, H. Ryu, F. Saied, M. Prada, M. Korkusinski, T. B. Boykin, and R. Rahman, IEEE Trans. Electron Devices **54**, 2079 (2007).
[27]S. Steiger, M. Povolotskyi, H.-H. Park, T. Kubis, and G. Klimeck, IEEE Trans. Nanotechnol. **10**, 1464 (2011).
[28]C. Robert, C. Cornet, K. Pereira da Silva, P. Turban, S. Mauger, T. Nguyen Thanh, J. Even, J. M. Jancu, M. Perrin, H. Folliot, T. Rohel, S. Tricot, A. Balocchi, P. Barate, X. Marie, P. M. Koenraad, M. I. Alonso, A. R. Goi, N. Bertru, O. Durand, and A. Le Corre, in *Proceedings of International Conference on Indium Phosphide and Related Materials (IPRM)* (2013), pp. 1–2.
[29]P. N. Keating, Phys. Rev. **145**, 637 (1966).

[30]I. Vurgaftman, J. R. Meyer, and L. R. Ram-Mohan, J. Appl. Phys. **89**, 5815 (2001).
[31]M. Zieliński, Phys. Rev. B **86**, 115424 (2012).
[32]J. Bardeen and W. Shockley, Phys. Rev. **80**, 72 (1950).
[33]G. L. Bir and G. E. Pikus, *Symmetry and Strain-Induces Effects in Semiconductors* (Israel Program for Scientific Translations, 1974).
[34]D. S. Watkins, *The Matrix Eigenvalue Problem: GR and Krylov Subspace Methods* (SIAM, 2007).
[35]L.-W. Wang and A. Zunger, J. Chem. Phys. **100**, 2394 (1994).
[36]A. Canning, L. W. Wang, A. Williamson, and A. Zunger, J. Comput. Phys. **160**, 29 (2000).
[37]A. J. Williamson, A. Franceschetti, H. Fu, L. W. Wang, and A. Zunger, J. Electron Mater. **28**, 414 (1999).
[38]A. J. Williamson, A. Zunger, and A. Canning, Phys. Rev. B **57**, R4253 (1998).
[39]V. Popescu and A. Zunger, Phys. Rev. B **84**, 125315 (2011).
[40]A. I. Yakimov, N. P. Stepina, A. V. Dvurechenskii, A. I. Nikiforov, and A. V. Nenashev, Phys. Rev. B **63**, 045312 (2001).
[41]M. Brehm, T. Suzuki, T. Fromherz, Z. Zhong, N. Hrauda, F. Hackl, J. Stangl, F. Schäffler, and G. Bauer, New J. Phys. **11**, 063021 (2009).
[42]M. El Kurdi, S. Sauvage, G. Fishman, and P. Boucaud, Phys. Rev. B **73**, 195327 (2006).
[43]K. Gradkowski, N. Pavarelli, T. J. Ochalski, D. P. Williams, J. Tatebayashi, G. Huyet, E. P. O'Reilly, and D. L. Huffaker, Appl. Phys. Lett. **95**, 061102 (2009).
[44]A. R. Goñi, C. Kristukat, F. Hatami, S. Dreßler, W. T. Masselink, and C. Thomsen, Phys. Rev. B **67**, 075306 (2003).
[45]A. R. Goñi, K. Syassen, K. Strössner, and M. Cardona, Phys. Rev. B **39**, 3178 (1989).
[46]S. L. Chuang, *Physics of Optoelectronic Devices* (John Wiley & Sons, Incorporated, 1995).